Nuclear Instruments and Methods in Physics Research A ∎ (∎∎∎∎) ∎∎∎–∎∎∎

Contents lists available at ScienceDirect

Nuclear Instruments and Methods in Physics Research A

journal homepage: www.elsevier.com/locate/nima

Large magnetic shielding factor measured by nonlinear magneto-optical rotation

J.W. Martin [a,b,*], R.R. Mammei [a,b], W. Klassen [a,b], C. Cerasani [a], T. Andalib [b], C.P. Bidinosti [a,b], M. Lang [b], D. Ostapchuk [a]

[a] Physics Department, The University of Winnipeg, 515 Portage Avenue, Winnipeg, MB, Canada R3B 2E9
[b] Department of Physics and Astronomy, University of Manitoba, Winnipeg, MB, Canada R3T 2N2

ARTICLE INFO

Article history:
Received 7 November 2014
Received in revised form
24 December 2014
Accepted 2 January 2015

Keywords:
Magnetometer
Magnetic shielding
Neutron electric dipole moment
Nonlinear magneto-optical rotation

ABSTRACT

A passive magnetic shield was designed and constructed for magnetometer tests for the future neutron electric dipole moment experiment at TRIUMF. The axial shielding factor of the magnetic shield was measured using a magnetometer based on non-linear magneto-optical rotation of the plane of polarized laser light upon passage through a paraffin-coated vapor cell containing natural Rb at room temperature. The laser was tuned to the Rb D1 line, near the ^{85}Rb $F=2\rightarrow2,3$ transition. The shielding factor was measured by applying an axial field externally and measuring the magnetic field internally using the magnetometer. The axial shielding factor was determined to be $(1.3\pm0.1)\times10^{7}$, from an applied axial field of 1.45 μT in the background of Earth's magnetic field.

1. Introduction

The next generation of neutron electric dipole moment (EDM) experiments aims to measure the EDM d_n with proposed precision $\delta d_n \lesssim 10^{-27}$ e − cm [1–9]. In the previous best experiment [10], which discovered $d_n < 2.9\times10^{-26}$ e − cm, effects related to magnetic field homogeneity and instability were found to dominate the systematic error. A detailed understanding of passive and active magnetic shielding, magnetic field generation within shielded volumes, and precision magnetometry is expected to be crucial to achieve the systematic error goals for the next generation of experiments. Much of the R&D effort for these experiments is focused on careful design and testing of various magnetic shield geometries with precision magnetometers [11–15].

Our work focused on the creation of a new small-scale magnetic shield designed primarily for magnetometer tests for our future nEDM experiment at TRIUMF. Within the shield, we prepared a magnetometer based on non-linear magneto-optical rotation (NMOR). NMOR results in a rotation of the plane of polarization of laser light resonant with atomic transitions in Rb vapor. In NMOR, the optical properties of the medium are modified by the laser light, resulting in nonlinear effects such as hole-burning and the creation of a coherent dark state [16]. The combined effect results in ultranarrow linewidths of ∼Hz, corresponding to projected field sensitivities at the few fT level [17]. The effect, which occurs near zero field, can be displaced to a non-zero field using either a frequency-modulated (FM) [18] or amplitude-modulated (AM) [19–21] pump beam, and a CW probe beam, and can in principle retain ∼fT precision [22]. At such precision, the technology is superior to fluxgate magnetometers, and rivals the precision of SQUID magnetometers, without the need for cryogenics. Recently, a three-axis NMOR-based magnetometer has been demonstrated [15].

Our magnetometer was based on the zero-field effect along a single axis. By calibrating the zero-field magnetometer using coils internal to the magnetic shield, we determined the axial magnetic shielding factor for fields applied by external coils. A key result of this work is that very large DC shielding factors could be measured in a small space, for small applied external fields (more than an order of magnitude smaller than Earth's field). Such measurements could not have been conducted using a conventional fluxgate magnetometer. The results validate our initial design goals for the magnetic shielding. The results also highlight the applicability of precision NMOR-based magnetometers in magnetically shielded environments, such as those that will be seen in future neutron EDM experiments.

2. Passive magnetic shield system

Analytical approximations exist for the transverse and axial shielding factors of completely closed and open finite multi-layered cylindrical shapes made of materials with high magnetic permeability μ

* Corresponding author at: Physics Department, The University of Winnipeg, 515 Portage Avenue, Winnipeg, MB, Canada R3B 2E9.
E-mail address: j.martin@uwinnipeg.ca (J.W. Martin).

http://dx.doi.org/10.1016/j.nima.2015.01.003
0168-9002/

[23–26]. Here transverse (axial) shielding implies a reduction in the externally applied magnetic field that is perpendicular (parallel) to the axis of concentric cylindrical shells. Closed-ended cylindrical structures have a higher axial shielding factor than open-ended concentric shells [23]. Shield structures often need apertures permitting access to the internal shielded volume for e.g. laser light, subatomic particles, and wires for field generation. Often cylindrical extensions, or "stovepipes", are situated around the apertures. Stovepipes generally may increase the shielding factor, however the optimum length is highly dependent on the design constraints and parameters of the shield structure. The shield used in this work was designed using a commercial finite element analysis (FEA) software package [27]. Special care was taken to design the apertures and stovepipes in the ends of the shield achieving as large as possible axial magnetic shielding factor.

2.1. Design constraints

The shield was designed in using FEA by requiring that the magnetic field within a region of interest (ROI) internal to the shield be as small as possible under application of an external axial field. For design purposes, the ROI was selected to be 4 in. (10.16 cm) long and 1 in. (2.54 cm) diameter, corresponding to the space inhabited by most magnetometers of interest. The innermost shield was required to be at least 4 in. (10.16 cm) in diameter and 8 in. (20.32 cm) long, in order to accommodate various coils as well as the magnetometers and support structures. The outermost shield diameter was required to be less than 12 in. (30.48 cm) to keep the shield small enough to rest on an optics table. All access to the inner shield was to be provided by a single $1\frac{1}{8}$ in. (2.86 cm) protrusion on each end to admit laser light along the axis (as well as cabling for field coils). Only the axial shielding factor was considered in designing the shield, because the axial shielding factor is generally smaller than the transverse shielding factor for this geometry.

The material to be used for the shield was fixed at 1/16 in. (0.159 cm) thick, since this material is readily available and cost effective. Both three- and four-layer shields were considered. Initial estimates of the axial shielding factor were conducted by comparing the results of the approximate axial shielding factors of Refs. [23]. A stovepipe geometry on the axial 2.86 cm protrusion in each shield layer was considered based on the analytical result found in Ref. [31] for the exponential decay of an axial field leaking into an open-ended cylinder.

A starting design based on these considerations was then implemented in the FEA simulation. The length L_i and radius R_i of each shielding layer i, the number of layers ($N=3$ or 4 where $1 \le i \le N$ and $i=1$ refers to the innermost shield), and the length of the stovepipe ℓ were allowed to vary in the simulation. The radii of the shields were constrained to obey $R_{i+1}/R_i = c$ where c is a constant independent of the layer. The length of each successive layer was constrained to follow $L_{i+1} = L_i + 2\ell + R_{i+1} - R_i$. Thus there is a gap between the end of a stovepipe and the next layer's lid of $\frac{1}{2}(R_{i+1} - R_i)$. This ensures sufficient space between the stovepipes and lids of each layer, i.e. the stovepipes are not nested. Other fractions of this gap were not considered. As expected based on simple estimation, the best results for the shielding factor were found for the larger number of shield layers $N=4$ and the value of c being as large as possible $c = (R_4/R_1)^{1/3} = 1.4$ so that $R_4 = 6$ in. if R_1 is constrained to be 2 in.

A somewhat surprising result was that shorter shields with shorter stovepipes were preferable, in that the additional length implied by longer stovepipes ultimately served only to make the shield longer, with a somewhat negative impact on the overall shielding factor. The FEA result is displayed graphically in Fig. 1. This was found to be qualitatively in agreement with recent work in Ref. [32].

Magnetic field homogeneity using a simple solenoidal internal coil design (reminiscent of the one described in Section 2.3) was also checked in the ROI, and confirmed that the 20.32 cm length of the innermost shield would be sufficient for sub-percent homogeneity over the ROI.

2.2. Final design and fabrication

The final design is shown in Fig. 2 and the dimensions as constructed were similar. The magnetic shield was fabricated and annealed by Ad-Vance Magnetics, Inc. [28]. The vendor informally suggested an effective DC permeability relative to that of free space $\mu_r \equiv \mu/\mu_0 = 20,000$ for the AD-MU-80 material used for the shield. Using this value in our FEA simulations implied an anticipated axial magnetic shielding factor of 1.1×10^7. Given that our goal is to employ such a shield in a near zero-field environment, the choice of a constant, DC value for μ_r in the simulations is well justified here.

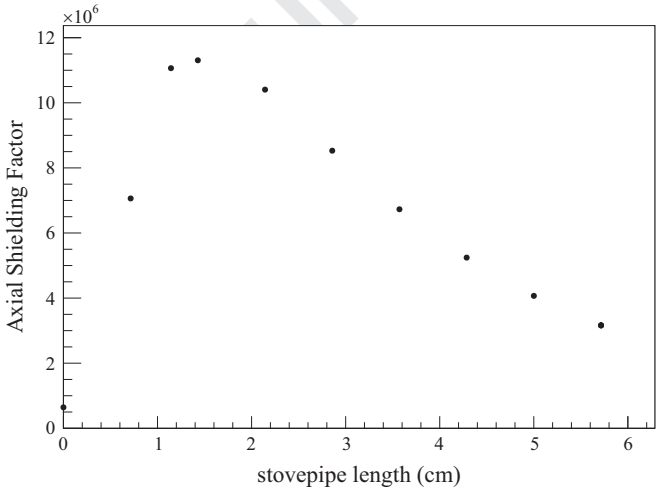

Fig. 1. FEA study of axial shielding factor vs. stovepipe length ℓ for a four-layer shield with radial dimension as in Fig. 2. A gap of $\frac{1}{2}(R_{i+1} - R_i)$ exists between each stovepipe and the subsequent shield, so that the stovepipes are fully contained by the next layer. Under these conditions, the axial shielding factor decreases as the stovepipe length (and therefore overall shield length) increases. The optimal stovepipe length is of order half the hole diameter.

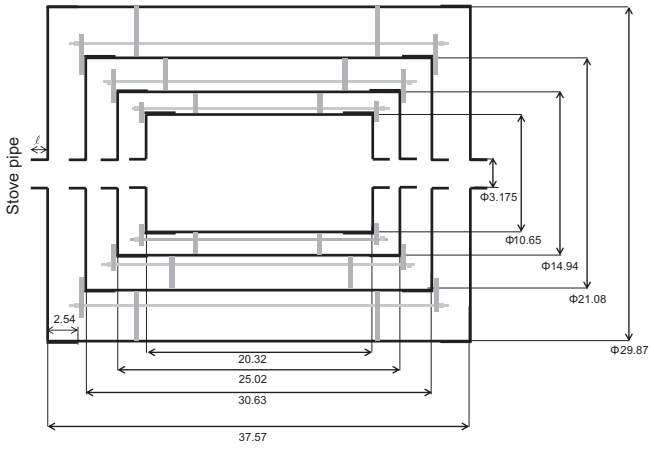

Fig. 2. Schematic diagram of the 4-layer magnetic shield (dimensions in cm). Outer diameters of the cylinders are shown, and dimensions are quoted in centimeters. The diameter of each endcap is larger by 0.1 cm to fit over its corresponding cylinder, extending 2.54 cm over the end of it. The hole diameter and stovepipe length for each endcap are the same. High density polyethylene spacers and nylon thread rods/nuts, shown in gray, hold the shields and end caps together.

Please cite this article as: J.W. Martin, et al., Nuclear Instruments & Methods in Physics Research A (2015), http://dx.doi.org/10.1016/j.nima.2015.01.003